J Mater Sci (2010) 45:6805–6811
DOI 10.1007/s10853-010-4778-8

Fabrication of hierarchical CdS microspheres assembled by nanowires: solid state electro-chemiluminescence in H_2O_2 solution

Zhen Fang · Xiu Lin · Yufeng Liu · Yueting Fan · Yinggui Zhu · Yonghong Ni · Xianwen Wei

Received: 28 January 2010 / Accepted: 17 July 2010 / Published online: 30 July 2010

Abstract Hierarchical CdS microspheres self-assembled by nanowires were synthesized via an ethylenediamine tetraacetate assisted solvothermal approach using cadmium chloride and L-cysteine as reaction agents. The phase structure, morphology, and optical properties of the products were investigated by X-ray powder diffraction, scanning electron microscopy, transmission electron microscopy, and electro-chemiluminescence, respectively. Studies showed that the final morphology of the products was strongly influenced by the concentration of ethylenediamine tetraacetate and reaction temperature. The as-prepared hierarchical CdS spheres could be a good candidate for a detective technology due to its high electro-chemiluminescence intensity.

Introduction

Recently, self-assembled hierarchical nanostructures with novel morphology and properties have attracted intensive attentions for its unique function in the development of advanced devices and systems. For instance, TiO_2 nanocolumn arrays [1], porous ZnO [2], flowerlike CeO_2 [3], metal sulfide, V_2O_5/TiO_2, $Au/Ag/Fe_3O_4$ have been synthesized by pulsed laser deposition, hydrothermal, microwave radiation, vapor deposition process, and self-assembled methods [4–9]. However, it is still a challenge to develop facile and effective route for the fabrication of hierarchical structure assembled with one-dimensional nanowire under mild condition.

As an important II–VI group semiconductor with a narrow band gap of 2.4 eV at room temperature, CdS has been widely studied for its various potential applications in photoelectric conversion in solar cells, light-emitting diodes for flat-panel displays, thin film transistors, and optical devices based on nonlinear properties [10–16]. During the past decades, many methods have been explored for the synthesis of CdS nanostructures, including solvothermal [17], hydrothermal [18, 19], thermal evaporation [20], template growth [21], and chemical vapor deposition [22, 23] routes. Among these methods, organic amine assisted solvothermal method is the most common one. Since ethylenediamine was used by Li et al. to synthesize one-dimensional CdS nanorods through solvothermal method, many efforts on the synthesis of CdS nanostructures via the same strategy had been reported [24–26]. In this work, we first used ethanolamine as solvent to replace ethylenediamine to synthesize hierarchical CdS microspheres for its low toxicity and good performance in the synthesis of hierarchical CdS nanostructures [27].

Experimental section

Preparation of hierarchical CdS microspheres: in this work, all of the reagents were analytical grade and used without further purification. In a typical synthesis, 1 mmol cadmium chloride ($CdCl_2 \cdot 2.5H_2O$) and 2 mmol L-cysteine ($C_3H_7O_2NS$) were dissolved, respectively, in 20 mL ethanolamine under stirring for 6 h to form a transparent solution. The two solutions were mixed together at room temperature. Then 3 mmol ethylenediamine tetraacetate (EDTA, $C_{10}H_{14}N_2O_8 \cdot 2H_2O$) was added to the mixture and

Z. Fang (✉) · X. Lin · Y. Liu · Y. Fan · Y. Zhu · Y. Ni · X. Wei
Anhui Key Laboratory of Functional Molecular Solids and College of Chemistry and Materials Science, Anhui Normal University, Wuhu 241000, People's Republic of China
e-mail: fzfscn@mail.ahnu.edu.cn

stirred for another 1 h until EDTA was homogeneously dissolved in the solution. The resulting solution transferred into a 60 mL Teflon-lined stainless steel autoclave which was sealed and heated at 150 °C for 6 h. The yellow precipitate was collected by filtration and washed with distilled water and absolute ethanol for several times. The yielded product was then dried in vacuum at 60 °C for 6 h and kept for further characterizations. In the comparative experiments, the reaction time and reaction temperature were altered, respectively, while keeping other conditions constant.

Characterizations

X-ray powder diffraction (XRD) patterns of the samples were characterized using a Shimadzu XRD-6000 with Cu Kα radiation. For the element analysis of the products, energy-dispersive spectrometer (EDS) was measured by scanning electron microscopy (SEM, Hitachi S-4800) with Horiba EMAX Energy EX-250. Morphology, structure, and size of as-synthesized products were obtained on SEM and high-resolution transmission electron microscopy (HRTEM, JEOL-2010). The electro-chemiluminescence (ECL) of products was performed on a MPI-E ECL analyzer system (Xi'an Remax Electronic Science & Technology Co. Ltd.). Cyclic voltammetry (CV) was demonstrated on a CHI660C electrochemical analyzer (Chenhua Inc.). All ECL measurements were performed on a standard three-electrode set-up (3 mm glassy carbon electrode (GCE) as working electrode, Ag/AgCl saturated KCl as reference electrode, Pt as counter electrode). 10 mg of the products was added into 10 mL acetone and dispersed by ultrasonic, then 10 μL mixing solution was dropped on electrode surface to form films while acetone volatilization. The ECL-potential curve for the hierarchical CdS spheres was obtained in phosphate buffer solutions (PBS, pH = 9.0) solutions containing 10 mmol H_2O_2 and the working voltage of the photomultiplier tube (PMT) was intercalated at 800 V. The luminescence intensity with the working electrode current was observed in the potentials ranging from −1.5 to 0 V at a scan rate of 100 mV/s.

Results and discussions

Figure 1a is the XRD pattern of the as-prepared CdS sample. The reflection peaks can be indexed to be pure hexagonal wurtzite CdS with lattice parameters $a = 4.146$ Å and $c = 6.705$ Å, which is consistent with the standard data (JCPDS card number 41-1049). Compared with the standard diffraction pattern, no peaks of impurities were detected. In Fig. 1a, the relative intensity of the (002) diffraction peak is much stronger than the standard pattern, which indicates the products' tropism should be [001] direction. The element analysis of the products was also studied by EDS (Fig. 1b). The result indicates that products consist of Cd and S element with the atom ratio of Cd and S is about 1:1.03. (Cu element signal due to the use of Cu foils as the products substrate).

Figure 2a is the low-magnification SEM image of the obtained products, which shows that the product is composed of hierarchical uniform CdS microspheres with narrow diameter distributions of about 2 μm. Further observation of the sample shows that the microspheres are composed of uniform CdS nanowires (Fig. 2b). These nanowires, radiating from the center of the microspheres, have average diameters of about 15 nm and lengths of about 1 μm. The detailed structure of CdS spheres is further verified by TEM in Fig. 2c, which confirms that these nanowires are aligned in a radial way from the center to the surface of the microspheres. The HRTEM image of a single nanowire in Fig. 2d shows that the nanowire has clear lattice fringes with a lattice spacing of about 0.32 nm, corresponding to the spacing for the (002) planes of wurtzite CdS, indicating that the nanowire is a single crystal with preferential [0001] direction growth, and this

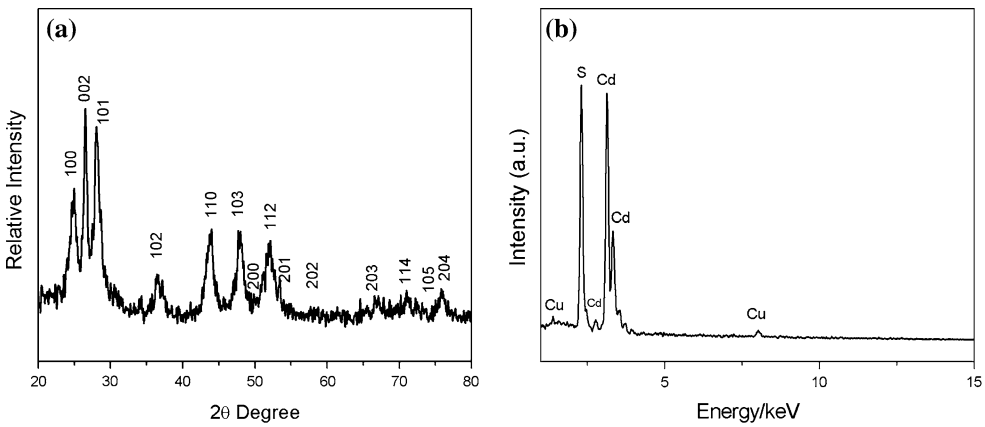

Fig. 1 **a** XRD patterns of as-prepared CdS samples. **b** EDS of hierarchical CdS spheres

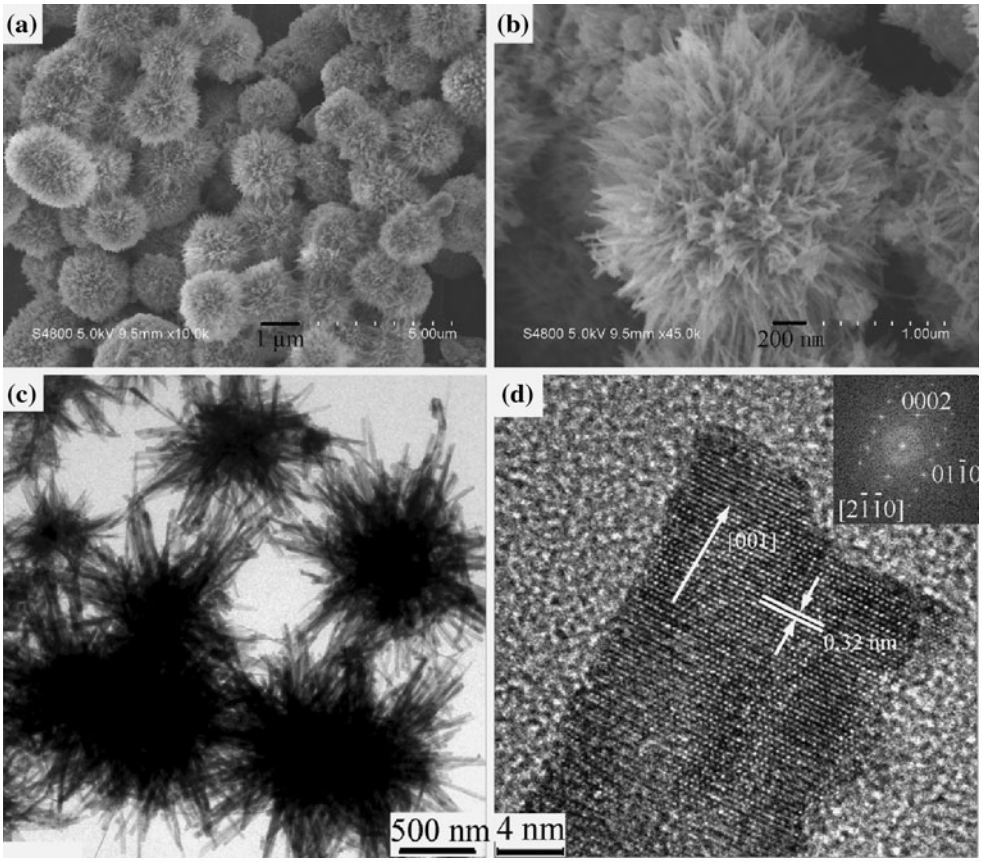

Fig. 2 FESEM images of the hierarchical CdS nanostructures. **a** Low resolution SEM image of hierarchical CdS spheres; **b** high-resolution SEM image of a single hierarchical CdS sphere. **c** TEM image of the hierarchical CdS nanostructures; **d** HRTEM image of the hierarchical CdS nanostructures. The *inset* is the Fourier transform electron diffraction patterns

agrees well with the XRD result. The fast Fourier transform (FFT) pattern (the inset of Fig. 2d) also indicates that the nanowires grow along $[2\bar{1}\,\bar{1}0]$ zone axis.

The former results suggested that L-cysteine can coordinate to Cd^{2+} to form $[Cd(cysteine)_2]^{2+}$ complex and then decomposes to form the initial CdS nuclei under solvothermal condition [28]. The FT-IR spectra of L-cysteine and the products collected at different reaction time are shown in Fig. 3a. The absorption bands of L-cysteine centering at 3180–2981 cm^{-1}, 2552 cm^{-1}, 1595 cm^{-1}, and 1066 cm^{-1} are assigned to the $\nu(NH_2)$ (asymmetric and symmetric stretching modes), ν(SH) (stretching modes), ν(C=O) (stretching modes) and δ(NH) (bending mode), respectively [29]. FT-IR of the products collected after solvothermal treatment for 1 h exhibit absorption band of ν(C=O), δ(NH), and other bonds which observed in pure L-cysteine. However, the absorption band of ν(SH) was disappeared for the deprotonation and coordination through the sulfur [30]. (The broad ν(O–H) at $\sim$3400 cm^{-1} come from the trace amount of water in the products.) Along with the reaction time increases, the absorption band becomes weaker and weaker (Fig. 3a). The result indicates the decomposition of $[Cd(cysteine)_2]^{2+}$ complex and the formation of inorganic products. Figure 3b is the XRD pattern of the product obtained at different stage. The reaction products obtained after 1 h have a poor crystallinity. Along with the reaction time prolong, the crystallinity improved, which may indicates the growth of CdS nanowires. UV–Vis absorption spectra of the products obtained at 1, 3, and 6 h display an absorption peak in 392, 486, and 488 nm (Fig. 3c), all absorption peaks show blue shift compared with that of bulk CdS [22]. The product obtained after reacting for 1 h exhibit stronger quantum size effect compared with other samples, which indicates the smaller particle size of CdS crystals obtained at initial reaction. Both XRD and UV–Vis absorption spectra results illuminated the step-by-step growth of CdS crystals.

TEM study shows that the precipitation obtained at the first 1 h was mainly composed of incompact spheres being composed of CdS nanoparticles (Fig. 4a). Along with the reaction proceeding, hierarchical CdS microspheres were formed at the expending of CdS nanoparticles (Fig. 4b). On the basis of the experimental results mentioned above (IR, XRD, UV, and TEM), a solid–solution–solid process is

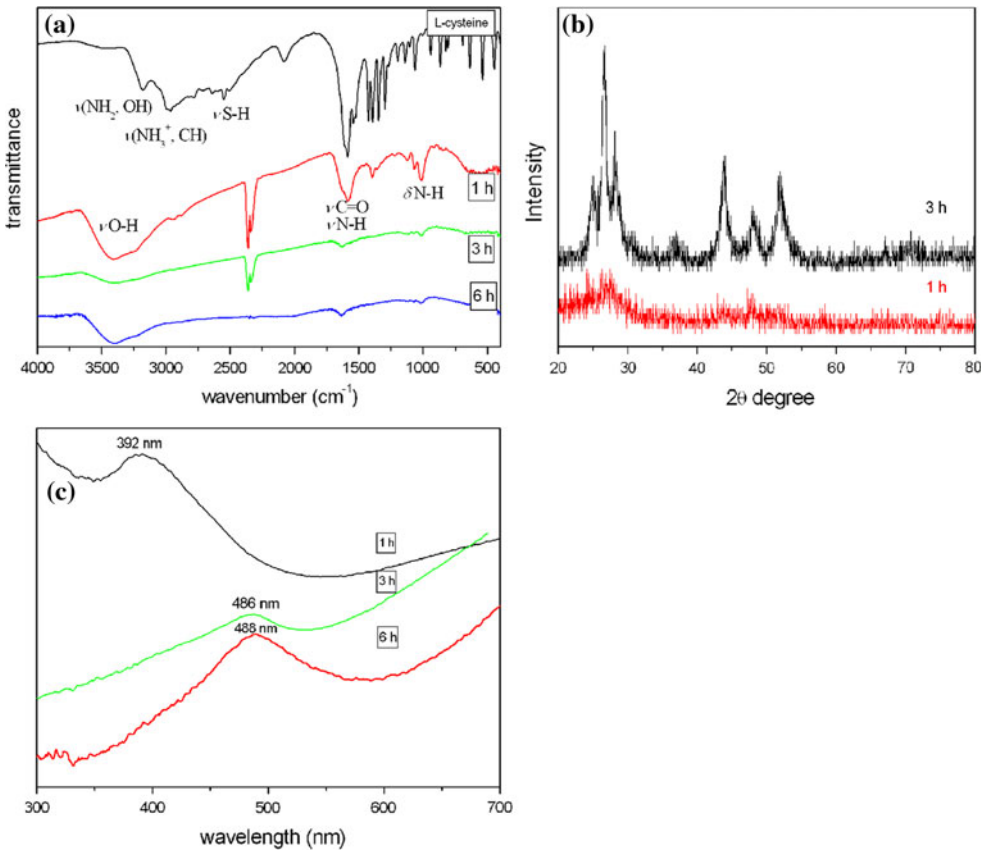

Fig. 3 **a** IR spectra; **b** XRD pattern; and **c** UV–Vis absorption spectra of the products at different reaction time

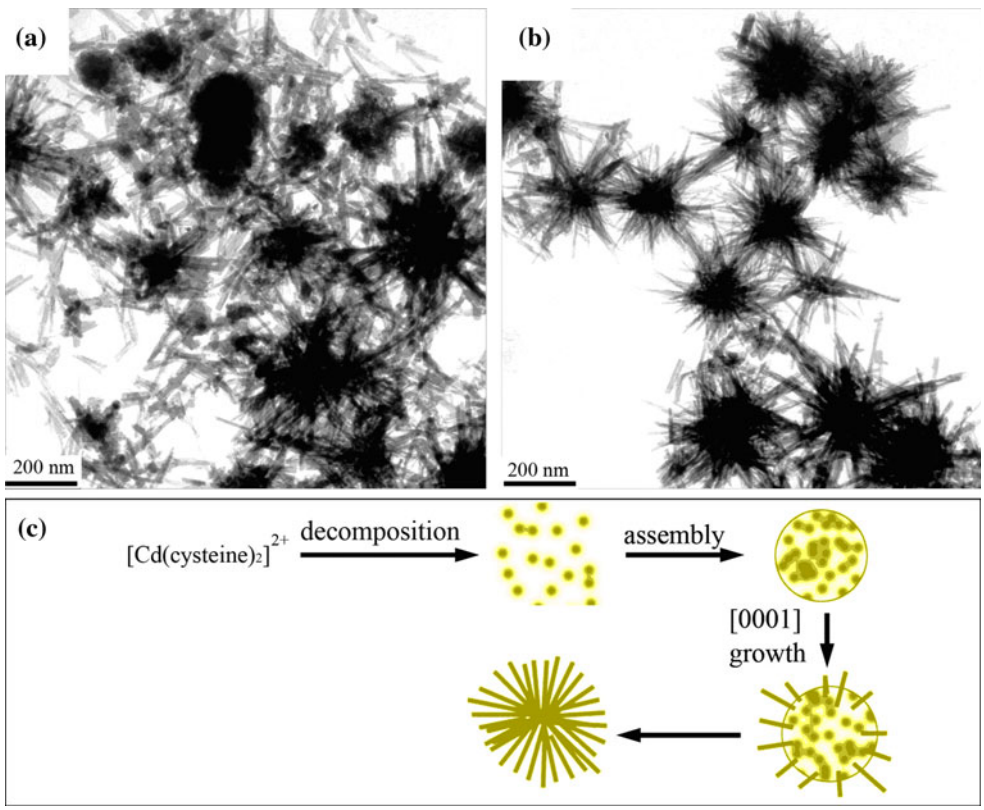

Fig. 4 TEM images of the samples synthesized at 150 °C for different reaction times: **a** 1 h; **b** 3 h. **c** schematic formation process of the hierarchical microspheres

proposed to illuminate the formation mechanism of the hierarchical structure. As shown in Fig. 4c, $[Cd(cysteine)_2]^{2+}$ complex decomposed to release CdS nuclei at a given temperature. To reduce total surface energy, the nuclei aggregated to form the incompact spheres in the first step. The formation of the incompact spheres is crucial in the whole synthetical process, because they served as substrate for the subsequent deposition of CdS nuclei. Finally, the urchin like CdS microspheres were formed with the expense of CdS nuclei decomposed from $[Cd(cysteine)_2]^{2+}$ complex.

As demonstrated by Li et al. and other groups, the coordinating effect between Cd^{2+} and organic amine has strong influence on the formation of CdS nanostructures [17]. In our experiment, it is speculated that EDTA acts as coordinating molecular template just like amine. To evaluate the effect of EDTA, we also varied the quantity of EDTA to study the effect of the additional capping ligand. Figure 5a presents an SEM image of the product obtained using 1 mmol EDTA, while keeping other conditions constant with the typical synthesis. The resulting urchin-like CdS microspheres was non-homogeneous. The relatively low concentration of EDTA caused a decrease in coverage of the CdS nanowires. The incomplete coverage of EDTA could not effectively control the growth rate of CdS nanowires, and the microspheres became non-homogeneous. Increasing the quantity of EDTA to 6 mmol, the products are polydisperse nanorods as shown in Fig. 5c. The high concentration of EDTA might cause high coverage on CdS nuclei at initial stage and make them monodiperse. The monodisperse CdS nuclei lead to polydisperse CdS nanorods along with the reaction proceeding. Furthermore, the high coverage on CdS nuclei will make the preference growth of crystal plane of CdS. XRD results of the products show that the sample at the high concentration of EDTA has [0001] tropism (Fig. 5b, d).

To further elucidate the roles of reaction temperature, we studied other two experiments at 100 and 180 °C. In Fig. 6a and b, they show spherical CdS nanostructures formed at 100 °C, no nanowires are observed on its surface. It seemed that the relatively low reaction temperature could not provide enough kinetic energy for the anisotropic growth of CdS nanowires. XRD in Fig. 6c shows that the products are nearly amorphous. However, over-high temperatures should be favorable for the formation of hierarchical microspheres. When the reaction temperature was increased to 180 °C, well self-assembled hierarchical CdS spheres were synthesized (Fig. 6d, e). The diameters of the hierarchical CdS spheres were about from 2 to 4 μm, which are dramatically increased in comparison with those obtained at 150 °C. The high-resolution SEM image of the individual hierarchical CdS sphere in Fig. 6e clearly indicates the well-aligned nanowire arrays with longer size.

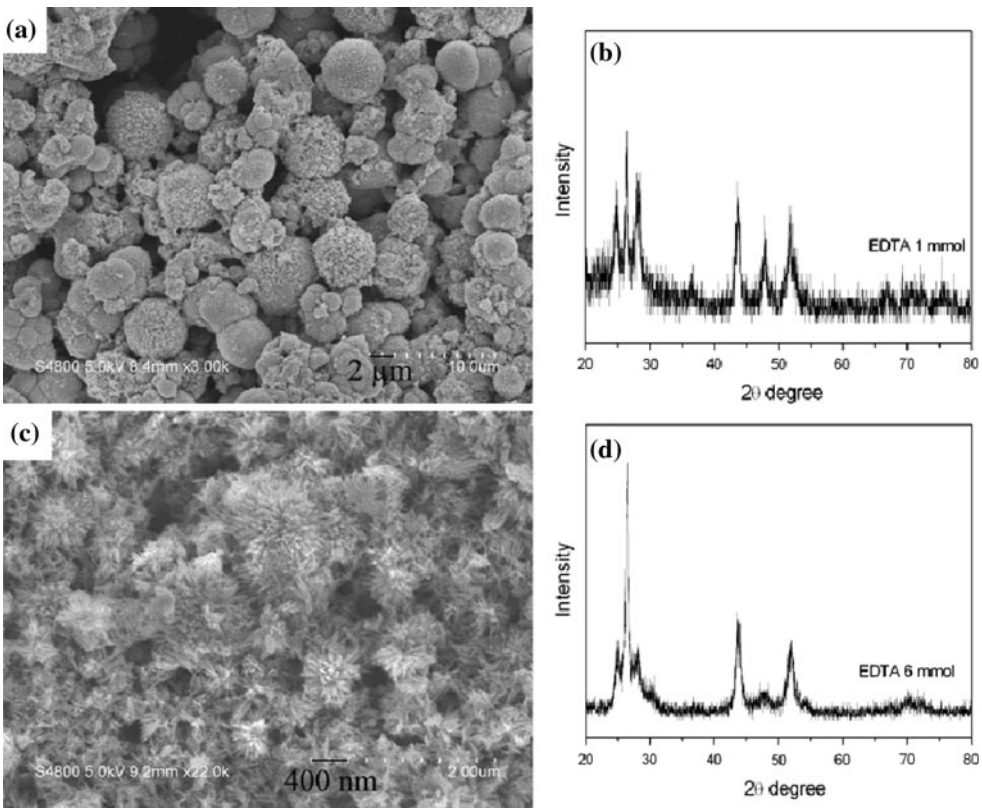

Fig. 5 FESEM image and XRD pattern of the samples synthesized with different quantity of EDTA: **a**, **b** 1 mmol; **c**, **d** 6 mmol

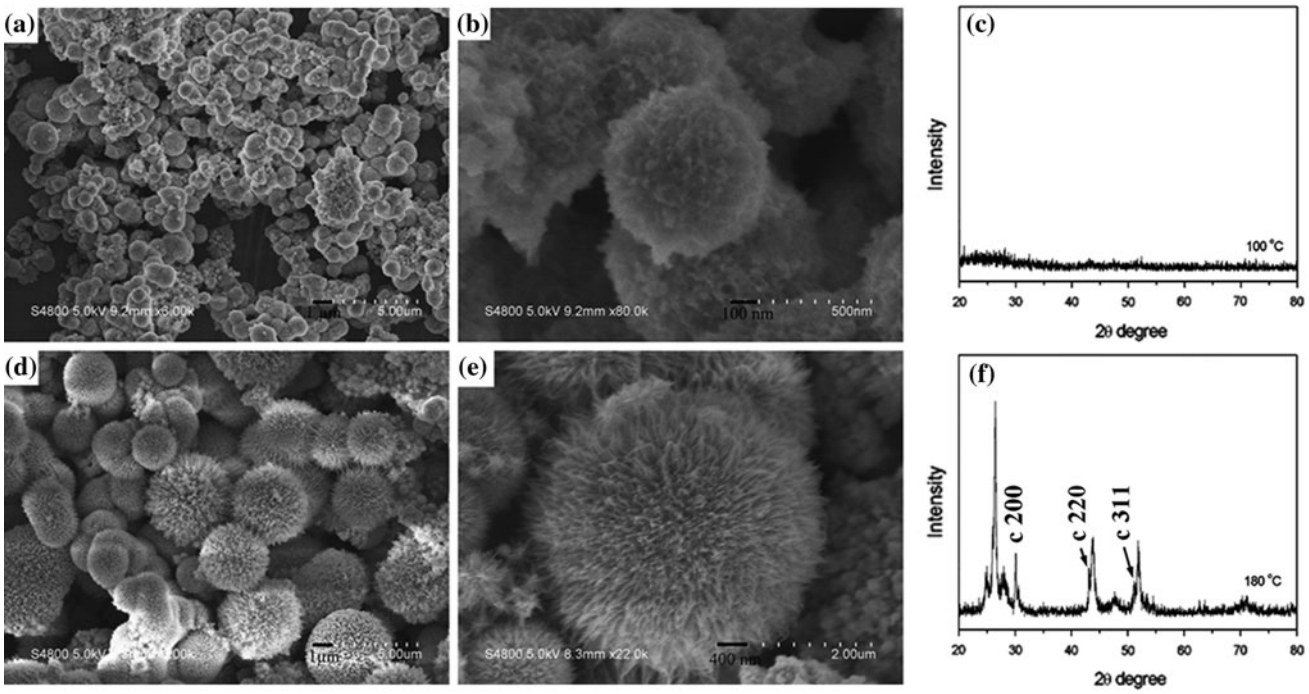

Fig. 6 FESEM images and XRD of the samples synthesized at different reaction temperatures. **a–c** 100 °C; **d–f** 180 °C. In figure (**f**), c denotes cubic CdS (JCPDS 75-1546)

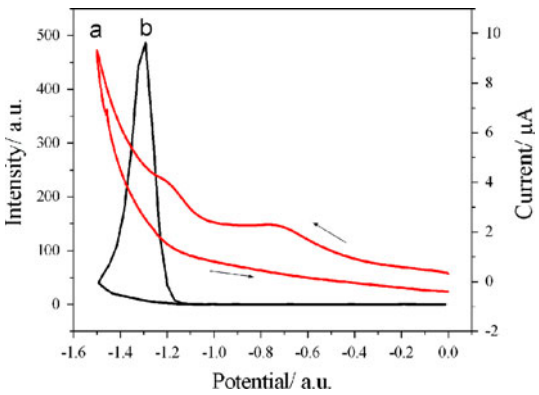

Fig. 7 *Line a*: the CV of the hierarchical CdS crystals film electrodes containing 10 mmol/L H_2O_2 at a scan rate of 100 mV/s. *Line b*: ECL curve of the hierarchical CdS crystals film electrodes in 0.1 mol/L PBS (pH 9.0) containing 10 mmol/L H_2O_2

XRD shows that the sample has good crystallinity with some cubic phase CdS impurity (Fig. 6f).

Cyclic voltammetry (CV) (line a in Fig. 7) indicates the cathodic peak current of the hierarchical CdS sphere is 9.5 μA. The ECL onset voltage (line b in Fig. 7) of the products is about −1.15 V, which consists with the CV result (−1.20 V). CdS is reduced by charge injection during electrode potential cycling and the electrogenerated reduced species (R^-) come into being (Eq. 1). The reduced species R^- is stable and collide with H_2O_2 to form an excited species (R*) with H_2O_2 being reduced into OH^- at the same time (Eq. 2). The unstable excited R* gives off light finally (Eq. 3) [31–33]:

$$CdS + 2e^- \rightarrow 2R^-, \quad (1)$$

$$2R^- + H_2O_2 \rightarrow 2R^* + 2OH^-, \quad (2)$$

$$nR^* \rightarrow CdS + hv. \quad (3)$$

The ECL-potential curve for the hierarchical CdS spheres shows a strong peak at −1.50 V and indicates a high ECL intensity of the products. According to the previous literature [7, 34, 35], the ECL emission depends on the surface properties and the presence of surface states. The high ECL intensity of the hierarchical CdS spheres is sure due to their unique morphology and will have potential value in analytical fields.

Conclusions

Hierarchical CdS microspheres have been synthesized by solvothermal method. The experimental results revealed that the morphologies of CdS microspheres were influenced by the concentration of EDTA, which act as coordinating molecular template. The hierarchical CdS nanostructures show a high ECL intensity, which may have potential applications in analytical and detection technologies.

Acknowledgements We are grateful for the financial supports from the National Natural Science Foundation of China (20701002), Science and Technological Fund of Anhui Province for Outstanding Youth (08040106834), and the Education Department of Anhui Province (no. 2006KJ006TD).

References

1. Li Y, Sasaki T, Shimizu Y, Koshizaki N (2008) J Am Chem Soc 130:14755
2. Xu F, Zhang P, Navrotsky A, Yuan ZY, Ren TZ, Halasa M, Su BL (2007) Chem Mater 19:5680
3. Yu RB, Yan L, Zheng P, Chen J, Xing XR (2008) J Phys Chem C 112:19896
4. Cao HL, Gong Q, Qian XF, Wang HL, Zai JT, Zhu ZK (2007) Cryst Growth Des 7:425
5. Zhang GQ, Lu XL, Wang W, Li XG (2007) Chem Mater 19:5207
6. Moore D, Ding Y, Wang ZL (2006) Angew Chem Int Ed 45:1
7. Fang Z, Wang XY, Shen JM, Lin X, Ni YH, Wei XW (2010) Cryst Growth Des 10:469
8. Ostermann R, Li D, Yin YD, Mccann JT, Xia YN (2006) Nano Lett 6:1297
9. Xu XX, Wang X, Nisar A, Liang X, Zhuang J, Hu S, Zhuang Y (2008) Adv Mater 20:3702
10. Wang ZL (2002) Adv Mater 12:1295
11. Zhao JL, Bardecker JA, Munro AM, Liu MS, Niu YH, Ding IK, Luo JD, Chen BQ, Jen AKY, Ginger DS (2006) Nano Lett 6:463
12. Yang C, Zhou XC, Wang LY, Tian XK, Wang YX, Pi ZB (2009) J Mater Sci 44:3015. doi:10.1007/s10853-009-3374-2
13. Barrelet CJ, Greytak AB, Lieber CM (2004) Nano Lett 4:1981
14. Hirai T, Bando Y, Komasawa I (2002) J Phys Chem B 106:8967
15. Peng XG, Schlamp MC, Kadavanich AV, Alivisatos AP (1997) J Am Chem Soc 119:7019
16. Xu WB, Wang YX, Xu RH, Liang S, Zhang GX, Yin DZ (2007) J Mater Sci 42:6942. doi:10.1007/s10853-006-1332-9
17. Li YD, Liao HW, Ding Y, Fan Y, Zhang Y, Qian YT (1999) Inorg Chem 38:1382
18. Nie QL, Yuan QL, Chen WX, Xu ZD (2004) J Cryst Growth 265:420
19. Zhang P, Gao L (2003) Langmuir 19:208
20. Shen GZ, Cho JH, Yoo JK, Yi GC, Lee CJ (2005) J Phys Chem B 109:9294
21. Lu W, Chen M, Wu LM (2008) J Colloid Interface Sci 324:220
22. Shen GZ, Lee CJ (2005) Cryst Growth Des 5:1085
23. Zheng J, Song XB, Chen N, Li XG (2008) Cryst Growth Des 8:1760
24. Li XH, Li JX, Li GD, Liu DP, Chen JS (2007) Chem Eur J 13:8754
25. Wang QQ, Xu G, Han GR (2006) Cryst Growth Des 6:1776
26. Sun FY, Yang Q, Zhao DL, Wu Y (2007) J Electron Mater 36:1567
27. Yao WT, Yu SH, Liu SJ, Chen JP, Liu XM, Li FQ (2006) J Phys Chem B 110:11704
28. Xiong SL, Xi BJ, Wang CM, Zou GF, Fei LF, Wang WZ, Qian YT (2007) Chem Eur J 13:3076
29. Chandrasekharan M, Udupa MR, Aravamudan G (1973) Inorg Chim Acta 7:88
30. Gai HD, Wu YS, Wu LL, Wang ZG, Shi YC, Jing M, Zou K (2008) Appl Phys A 91:69
31. Wang QQ, Zhao GL, Han GR (2004) Rare Metal Mater Eng 33:145
32. Ren T, Xu JZ, Tu YF, Xu S, Zhu JJ (2005) Electrochem Commun 7:5
33. Myung N, Lu XM, Johnston KP, Bard AJ (2004) Nano Lett 4:183
34. Bae Y, Myung N, Bard AJ (2004) Nano Lett 4:1153
35. Ding SN, Xu JJ, Chen HY (2006) Chem Commun 3631